MEMS MONOLITHIC TRI-AXIS HIGH-SHOCK ACCELEROMETERS WITH MHz-LEVEL ULTRA-HIGH RESONANT FREQUENCY

Hongshuo Zou[1,2], Fang Chen[1], Jiachou Wang[1], Haifei Bao[1], and Xinxin Li[1,2]

[1] State Key Lab of Transducer Technology, Shanghai Institute of Microsystem and Information Technology, Chinese Academy of Sciences, 865 Changning Road, Shanghai 200050, CHINA

2 University of the Chinese Academy of Sciences, Beijing 100049, China

ABSTRACT

This paper reports a novel structure for monolithically integrated tri-axis high-shock accelerometer. All the tri-axial sensors feature ultra-high resonant frequencies, in which the *Z*-axis accelerometer is no longer a shorter board in design compared to its in-plane X- and Y-axis counterparts. The axially compressed/stretched tiny-beams are connected into Wheatstone-bridge for piezoresistive detection. Processed in ordinary (111) wafers, a low-cost high-yield non-SOI fabrication technique is developed in this study for manufacturing the complicated structure that consists of the axially deformed micro-beams. Being tested under 10000g high-shock acceleration, every of the three accelerometers exhibit 1-2μV/g sensitivity and about 1.5MHz resonant frequency.

INTRODUCTION

In recent years, MEMS inertial sensors have been intensively studied. Bearing high performance and cheap price, some well developed MEMS accelerometers for automotive electronics and consumer electronics have been industrialized and widely applied in the market. As for high-g shock accelerometers for much higher measure range applications like collision test and structure destruction analysis, efforts have also been made to develop qualified sensors. However, so far the sensor performance still leaves a space for further improvement.

A dual-cantilever high-shock accelerometer fabricated in (111) wafer was proposed in the work of Ref. [1], where the chip size is small and only single-sided process is used to achieve high reliability and small sensor size. However, it is impossible for a cantilever-shaped accelerometer to simultaneously achieved high sensitivity and high resonant frequency. When sensitivity is high enough, normally the frequency bandwidth has to be sacrificed, i.e., the resultant frequency bandwidth is narrow. A monolithic tri-axis piezoresistive high-shock accelerometer was ever proposed, where the axially stressed tiny beams were adopted in *XY*-axis structure to improve the resonant frequency to about 300kHz [2]. Unfortunately its *Z*-axis sensing structure still used the old structural design [3], thus, the *Z*-axis performance was much worse than the other two axes. The work in [4] utilized a partly clamped plate to deflect under shock and the four piezoresistive beams were designed in axial stretch or compression for differential piezoresistive signal readout. In that way the resonant frequency of the formed single-axis high-shock sensor was increased to MHz level. Then the same group reported some refinement work for X-Y dual-axis accelerometers and outlined a plan of *Z*-axis accelerometer in [5], where the much lower 0.5MHz resonant frequency than that of the X-Y ones was expected. Being inferred from the contexts of [4] and [5] where no fabrication details was given, a monolithic tri-axis high-frequency shock sensor by using that complicated structure is difficult to be fabricated.

In order to achieve a monolithic tri-axis high-frequency shock sensor, the (111)-wafer micromachining process in [1] is considered to be suitable for the axial-deformed beam structure. Such a (111) silicon micromachining process has recently been used for successful fabrication of axial-beam resonant chemical sensors [6]. In this work we just try to use the (111)-wafer process to monolithically fabricate the wanted high-frequency tri-axis shock accelerometers.

Compared with traditional tri-axis shock sensors that were formed by assembling three discrete components into one packaging, monolithic tri-axis sensors are advantageous in miniaturization and ensuring the three axes being precisely perpendicular to each other. Besides, the monolithic scheme helps to secure uniform performance among the tri-axis elements (e.g. temperature drift). Unfortunately, so far there has been no monolithic tri-axis high-shock accelerometer that exhibits high sensitivity and MHz-level resonant frequency for all the three axes. Normally the Z axis sensor is with much worse performance than the other two axes.

This study proposes a novel structure for monolithically integrated tri-axis high-shock accelerometers. All the tri-axial sensors feature ultra-high resonant-frequencies and, thus, ultra-wide bandwidths for detecting wide-band dynamic high-shock with low response distortion. By designing a special sensing structure, axially compressed/stretched tiny-beams (at wafer front-side) serve as piezoresistors and are connected into Wheatstone-bridge for signal readout. A low-cost high-yield process for the tri-axis micro-beam high-g accelerometer is herein specifically developed. The sensors are bulk-micromachined in an ordinary (111) wafers. Tested under 10000g high-shock acceleration and DC-5V power supply, each of the three accelerometers exhibits 1-2μV/g sensitivity and about 1.5MHz resonant frequency.

SENSOR DESIGN

Fig. 1(a) shows the front-side view of the designed tri-axis sensor in a (111) wafer. Located at the chip center, the novel structure *Z*-axis sensor consists of four axial-deformed tiny-beams, two mass-blocks and a connection plate. The four axial-deformed piezoresistive beams are transversely bridged cross three narrow deep trenches. Accordingly the backside view in Fig. 1(b) shows the two shallow islands (i.e. the two mass-blocks). Fig. 1(c) shows the magnified cross-sectional view of the *Z*-axis

sensing structure, with the cross-section cut along A-A' in Fig. 1(a). The connection plate is used to stiffen the spring by reinforcing the structure. Crossing over the two mass-blocks, the double-clamped connection plate is connected to the silicon substrate. When high-g acceleration perpendicular to the wafer surface is applied to the twin mass-blocks, they tend to move along Z axis. Due to the asymmetric boundary condition at the connection joints between the mass-blocks and the connection plate, the relative motion between the two mass-blocks results in tension or compression of the axial-deformed beams at different locations. In this way the out-of-plane acceleration is converted into in-plane beam deformation for piezoresistive detection. When the two beams at the central trench are stretched, the other two at the two side-trenches will be compressed, thereby forming differential Wheatstone-bridge output. The piezoresistive coefficients in (111) wafer are independent of orientation and herein <211> is chosen as the beam orientation just for ease of fabrication. The resonant frequency and sensitivity are mainly determined by the dimensions of the two mass-blocks and the axial-deformed beams, and the performance can also be adjusted by changing the thickness of the connection plate. Since the mass-block and the connection plate are very robust and the micro-beams are deformed axially, the Z-axis accelerometer exhibits both high resonant frequency and high sensitivity.

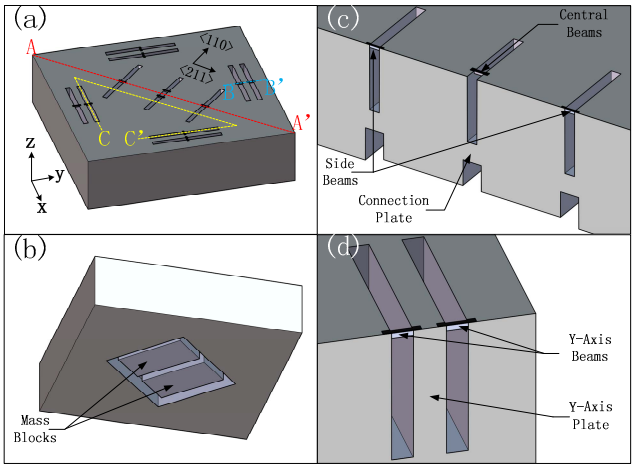

Fig.1: (a) 3D schematic of the tri-axis high-shock sensor chip. (b) Backside view of the sensor chip. (c) Locally magnified cross-sectional view of the Z-axis accelerometer. (d) Locally magnified cross-sectional view of the Y-axis (the same as X-axis) accelerometer.

The identical-shaped *X*-axis and *Y*-axis sensing structures are located at the surrounding area of the chip, with each having its two partly clamped plates laid face to face. Fig. 1(d) shows the cross section of the *Y*-axis structure, which is cut along B-B' of Fig. 1(a). Under shock along *Y*-axis, the partly clamped half-plate laterally deflects to cause axial stretch of two piezoresistive beams and axial compression (to the same degree) of the other two, thereby a full Wheatstone-bridge is formed for differential output. The angle bisector of <211> and <110> is chosen as the orientation of the beams to ensure that the *X*-axis structure is exactly the same as the *Y*-axis structure. The resonant frequency and sensitivity are mainly determined by the size of the partly clamped half-plate and the size of the axial-deformed beams.

To optimally design the sensitivity~frequency figure of merit ($S \cdot f^2$) to be equal among the three accelerometers, the sensor chip is analyzed by using FEM software. Fig. 2(a) shows the FEM simulated resonant frequencies of the tri-axis sensor, resulting in about 1.5MHz for all the three sensors. Under 100000*g* of *Z*-axis shock, the sensor deflection is shown in Fig. 2(b) and the axial-stress in the stretched and compressed beams are shown in Fig. 2(c) and 2(d). Because the boundary condition of the side beams is much stricter than that of the central beams, the deformation of the central beams are much larger than that of the side beams. The axial-stresses in the central beams, which contribute to most of the sensitivity, are about three times of the axial-stresses in the side beams. Under 100000g *X*-axis shock, the deflection is shown in Fig. 2(e) and the axial-stress distribution is shown in Fig. 2(f). The averaged axial-stress in *X*-axis beams is designed being almost equal to the averaged axial-stress in *Z*-axis beams (average value of central beams and side beams), which results in an equal sensitivity for each of the three sensors.

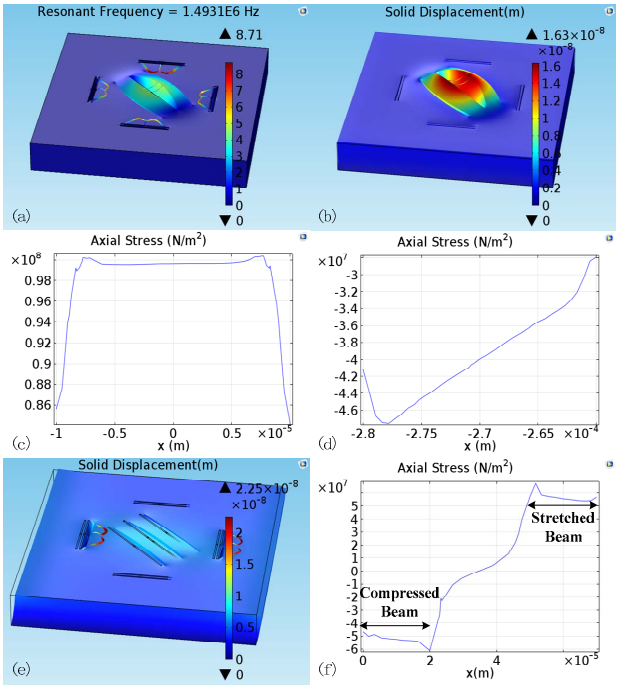

Fig.2: (a) Finite element simulation of resonant frequencies for the three accelerometers, resulting in about 1.5MHz for each of the three structures. (b) Deformation distribution under 100000g Z-axis acceleration. (c) Axial stress distribution along the central beams of the Z-axis accelerometer when 100000g Z-axis acceleration is applied. (d) Axial stress at the side beams of the Z-axis sensor under 100000g Z-axis acceleration. (e) Deformation under 100000g X-axis acceleration. (f) Opposite axial-stress at the two beams of the X-axis accelerometer under 100000g of Z-axis acceleration.

FABRICATION

It is really challenging to fabricate the axial-deformed

micro-beams, twin-mass blocks and partly clamped half-plate in a single wafer. To meet the requirement, a low-cost high-yield (111) silicon micromachining process is herein developed for the tri-axis high-g accelerometer. The sensors are bulk-micromachined in ordinary (111) wafers and the cross-sectional fabrication steps, cut along C-C' of Fig. 1(a) are listed in Fig. 3 and described as follows. In this way the formation of the twin mass-blocks can be shown at center and that of the micro-beams can be illustrated at the both sides. In the step (a), contact holes of the piezoresistors are opened by RIE in advance because the lithography on the flat wafer is much easier than on a deep trenches containing wafer [see the step (e) and later]. The depth of the shallow DRIE in (b) determines the thickness of the micro-beams. To form a gap for *Z*-axis movement, two steps of deep RIE are employed in the step (c). The exposed sidewalls of the beams are not (111) plane, thus, they need to be coated by LPCVD SiO_2 in the step (d). After deep trench etching in the step (e), the partly clamped half-plates and the mass-blocks are formed. In the step (f), the etching time is quite short (<10min) because the axial-deformed beams are very tiny (width<3μm). The thickness loss of the partly clamped half-plates (about 3μm lost from about 30μm total thickness) must be considered in design. The surfaces of the partly clamped half-plates of the *X*- and *Y*-axis accelerometers are either (2, $1+3^{1/2}$, $1-3^{1/2}$) or (2, $1-3^{1/2}$, $1+3^{1/2}$), which ensures that the etching conditions for the *X*- and *Y*-axis structures are the same. The redundant SiO_2 is removed in the step (g) to ensure the mechanical properties of the micro-beams. Electrical interconnection is realized by Al sputtering and patterning in the step (h).

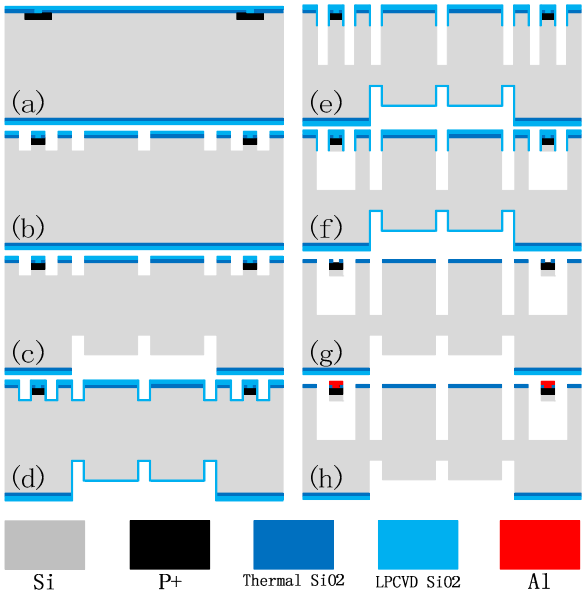

Fig.3: Cross-sectional process steps in N-type (111) wafers, cut along C-C' in Fig. 1(a). (a) Thermal oxidation , P^+ doping for piezoresistors, RIE for contact holes, TEOS LPCVD. (b) Relatively shallow deep-RIE for the micro-beams. (c) Two-step backside deep-RIE for the mass-blocks. (d) TEOS LPCVD for protection the side-wall of the beams. (e) Deepr trench etching. (f) TMAH etch to free the beams. (g) HF etching to remove redundant SiO_2. (h) Al metallization for electrical interconnection.

The fabricated tri-axis high-*g* accelerometer is shown in Fig. 4(a). The chip size is about 3.5mm×3.5mm. The axial-deformed beams are shown in the close-up views of Figs. 4(b) and 4(c). The cross-sectional size of the beam is 3μm×3μm and a high size uniformity is achieved among different micro-beams. The reason lies in that, the bottom of the micro-beam is (111) surface, towards which the TMAH etching rate to silicon is negligible and the other sidewall surfaces of the beam are well protected from etch by using SiO_2.

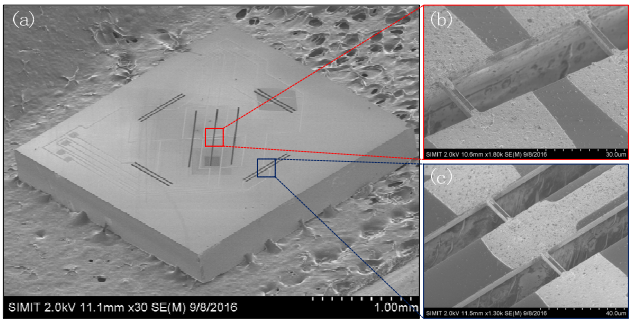

Fig.4: (a) SEM image of the 3.5mm×3.5mm sensor. (b) Magnified central beams of the Z-axis sensor. (c) Magnified axial-beams of the X-axis sensor.

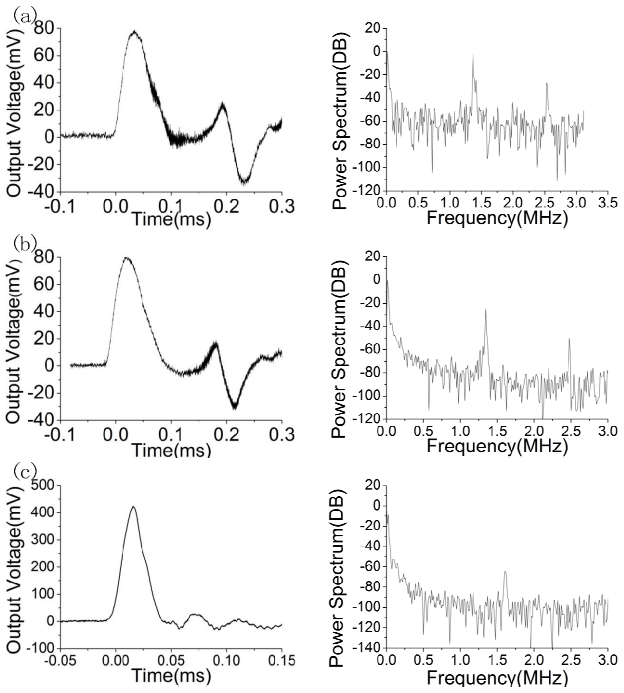

Fig.5: High-shock testing results. The output and the frequency-domain response of the X-, Y- and Z-axis sensors are shown in (a), (b) and (c), respectively.

TESTING RESULTS

The sensor chip is packaged in a ceramic envelope. A steel bar dropping hammer system is used to test the accelerometers [7]. With given output voltage V(t), amplification times of the circuit A and collision time Δt, the sensitivity of the sensor can be calculated as

$$S = \frac{\int_0^{\Delta t} V(t)dt}{2A\sqrt{2gH}} \qquad (1)$$

The resonant frequency can be obtained by fast Fourier transformation to the output data over the shocking time.

The testing results of the *Z*-axis high-shock accelerometer are shown in Fig. 5(c), exhibiting the high resonant frequency of 1.61MHz and high-sensitivity of 2μV/g (the full measure-range is designed for 100000*g*). Figs. 5(a) and 5(b) shows the similar testing results for the *X*-axis and *Y*-axis sensors, respectively. Their resonant frequencies are both about 1.37MHz and the sensitivity is about 1.1V/g. The output curve of the *Z*-axis accelerometer is a little different from the other two, which is partly due to the used different dropping steel bars and partly originated from the simple package.

CONCLUSIONS

MEMS monolithic tri-axis high-shock accelerometers with MHz level resonant frequency are reported in this paper. A novel structure for high-performance tri-axis accelerometers is proposed and analyzed. A low-cost high-yield (111) silicon micromachining process is developed for the micro-beam high-g accelerometers. The tested results show 1-2μV/g sensitivity and about 1.5MHz resonant frequency for the three-axis sensors, thereby well proving the novel structure design.

ACKNOWLEDGMENTS

The research is supported by the Project of Shanghai Science and Technology Commission (14521106100), the Chinese 863 Project (2015AA043502) and the NSFC Project (61674160, 51205388, 61321492).

REFERENCES

[1] J. Wang, X. Li, "A high-performance dual-cantilever high-shock accelerometer single-sided micromachined in (111) silicon wafers", *J Microelectromech. Syst.*, vol.19, pp. 1515-1520, 2010.

[2] P. Dong, X. Li, H. Yang, H. Bao, W. Zhou, S. Li, S. Feng, "High-performance monolithic triaxial piezoresistive shock accelerometers", *Sens. Actuators A*, vol.141, pp. 339-346, 2008.

[3] Z. Wang, D. Zong, D. Lu, B. Xiong, X. Li, Y. Wang, "A silicon micromachined shock accelerometer with twin-mass-plate structure", *Sens. Actuators A*, vol.107, pp. 50-56, 2003.

[4] R. Kuells, S. Nau, M. Salk, et al, "Novel piezoresistive high- g, accelerometer geometry with very high sensitivity-bandwidth product", *Sens. Actuators A*, vol.182, pp. 41-48, 2012.

[5] R. Kuells, S. Nau, M. Salk, K. Thoma, "Design of a 1D and 3D monolithically integrated piezoresistive MEMS high-g accelerometer" *Digest Tech. Papers Inertial Sensors and Systems '14 Symposium*， California， Feb 25-26, 2014, pp. 1-4.

[6] F. Yu， J. Wang， P. Xu， X. Li, "A Tri-Beam Dog-Bone Resonant Sensor With High-, in Liquid for Disposable Test-Strip Detection of Analyte Droplet", *J Microelectromech. Syst.*, vol.25, pp. 244-251, 2016.

[7] T. G. Brown and B. S. Davis, "Dynamic high-g loading of MEMS sensors: Ground and flight testing," *Proc. SPIE*, vol. 3512, pp. 228–235, 1998.

CONTACT

* Xinxin Li, tel: +86-21-62131794; *xxli@mail.sim.ac.cn*